

Stability and von Zeipel-Lidov-Kozai effect of circumbinary disks in the Galactic Center

Yannick Badoux^{1*†}, Lucas Pouw^{1*†} and Tim van der Vuerst^{1*†}

^{1*}Leiden Observatory, Leiden University, PO Box 9513, Leiden, 2300 RA, The Netherlands.

*Corresponding author(s). E-mail(s): badoux@strw.leidenuniv.nl; pouw@strw.leidenuniv.nl; vdvuerst@strw.leidenuniv.nl;

[†]These authors contributed equally to this work.

Abstract

Recently, the detection of an S-star binary system has been reported through a periodic variation in its Brackett γ emission (Peißker et al., 2024). This variation may be caused by periodic interactions with a circumbinary accretion disk. The stability of such a system is uncertain, given the dynamic nature of the Galactic Center. Therefore, we present Bridged gravito-hydrodynamic simulations of a stellar binary system with a circumbinary disk that is altogether orbiting a supermassive black hole. We find that there exists a quasi-stable configuration for a circumbinary disk, in which periodic disk mass loss is driven by von Zeipel-Lidov-Kozai oscillations.

Keywords: Galaxy: nucleus, Galaxy: kinematics and dynamics, methods: numerical, stars: variables: T Tauri, Herbig Ae/Be

1 Introduction

Recently, Peißker et al. (2024) reported the detection of an S-star binary system, called D9. The primary of D9 is found to be a Herbig Ae star and therefore has a circumstellar disk. The secondary would be a T-Tauri star. The binary nature of D9 was hypothesized because of the periodicity in its Brackett γ (Br γ) emission. Noting that Br γ emission is associated with accretion processes of Herbig Ae/Be stars and T-Tauri stars (Muzerolle et al., 1998; Grant et al., 2022), the authors propose that this periodicity originates from interactions of the secondary with an accretion disk.

However, the location of the measured disk component of D9 is uncertain, because a circumbinary disk may obscure the circumprimary disk. A hint to its location may be offered by the inferred low disk mass of $M_{\text{disk}} = 1.61 \cdot 10^{-6} M_{\odot}$. The authors speculate that this low mass may be explained by a possible formation scenario of the system, in which a molecular cloud migrates towards Sgr A* during which D9 could have formed. Subsequently, a circumbinary disk is formed and photoevaporates, giving rise to its low mass.

Additionally, [Peißker et al. \(2024\)](#) note that a merger of D9 may soon occur, because of the von Zeipel-Lidov-Kozai (vZLK) mechanism ([von Zeipel, 1910](#); [Lidov, 1962](#); [Kozai, 1962](#)) driving the binary eccentricity up and thus decreasing the binary separation at periaapse.

Thus, D9 might have been observed at a particularly special time, when the binary has not yet merged and a circumbinary disk has not yet fully evaporated. Moreover, the system has neither been disrupted by the dynamical environment of the Galactic Center (GC), nor by the vZKL oscillations of the binary ([Franchini et al., 2019](#)).

This raises the question as to how likely the interpretation is of D9 as a stellar binary with a circumbinary disk. In this work, we investigate the possibility of a circumbinary disk surviving the dynamical environment of the GC. To this end, we simulate a binary system with a circumbinary disk that is altogether orbiting an SMBH.

The results of our simulations are shown in [sect. 2](#). The detailed setup of the code is laid out in [sect. 3](#). We discuss the results in [sect. 4](#) and summarize our conclusions in [sect. 5](#).

2 Results

2.1 Searching for stable radii

The dimensions of the D9 disk have not been estimated in [Peißker et al. \(2024\)](#). Therefore, we have performed multiple simulations with varying initial inner and outer disk radii. A detailed explanation of our choice of initial conditions can be found in [sect. 3.2](#).

The disk loses particles over time (see [Fig. 1](#)). We can distinguish three regimes in the graph of the number of bound particles over time:

1. Stable: no loss of particles
2. Unstable: loss of particles at a high rate
3. Quasi-stable: loss of particles in periodic bursts

In [Fig. 1](#), we also plot histograms of the radial distributions of disk particles in this quasi-stable state. From this plot, it can be seen that the disk has converged to the same radial mass distribution in all instances. This indicates that this is an equilibrium state for the disk.

To test this hypothesis, we run a simulation in which the initial disk radii are given by the bounds of the 68% confidence interval of this radial mass distribution. The median is 8.77 AU and standard deviation is 0.65 AU. Therefore, we choose $R_{\text{min}} = 8.12$ AU and $R_{\text{max}} = 9.42$ AU. The result is shown in [Fig. 2](#).

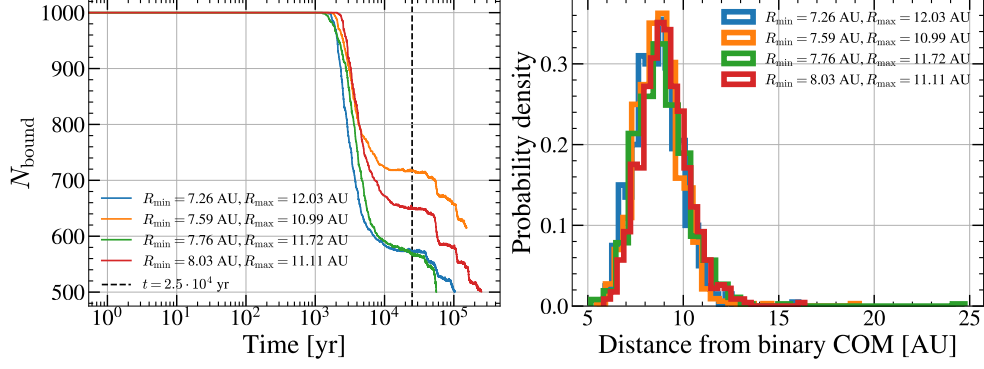


Fig. 1: *Left:* Four runs that have reached a quasi-stable plateau. *Right:* Radial distribution of disk particles in the plateau configuration at $t = 2.5 \cdot 10^4$.

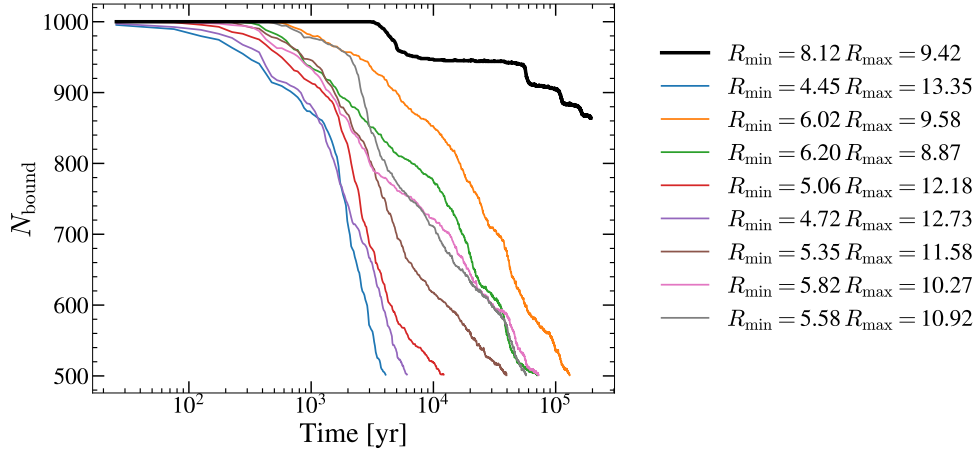


Fig. 2: The number of bound disk particles over time for different initial inner (R_{min}) and outer (R_{max}) disk radii.

Indeed, the stable phase of the disk has lasted significantly longer and the subsequent particle loss was less severe. This figure also shows that the rate at which particles become unbound is slower for smaller disks. Most disks in the runs plotted in this figure have not yet settled into the quasi-stable state, because the stopping condition is reached before that can happen. However, we postulate that most simulations would have otherwise converged to this state.

2.2 The von Zeipel-Lidov-Kozai effect

The initial conditions found allow the disk to survive for multiple vZLK timescales. In Fig. 3, we show the vZLK oscillations for three cases: the binary orbit¹ and the bound particle orbits of a circumbinary disk and a circumsingle disk. From this figure, we see that the disk particle orbits trace the oscillations of the binary. Moreover, these oscillations are visible in three spatial angles.

The circumsingle disk does not display these oscillations. This is because the disk quickly loses its flat structure as the disk particle orbits become more isotropic in the absence of a binary.

Finally, we note that the particle loss of the most stable disk in Fig. 2 has a periodicity similar to the observed vZLK timescale, indicating a causal relation.

3 Methods

3.1 Numerical Integrators

The dynamics of the binary system orbiting the SMBH is handled by the gravitational N-body code *Huayno* (Jänes et al., 2014). For a comparison with *Hermite* (Makino, 1991), see Appendix A. We will use *Huayno* as we deem its accuracy sufficient for our problem and it is faster than *Hermite*.

To simulate the dynamics of the disk, we use the Smoothed-Particle Hydrodynamics (SPH) code *Fi* (Hernquist and Katz, 1989; Gerritsen and Icke, 1997; Pelupessy et al., 2004). We set the *Fi* timestep to 1% of the binary period (~ 4 days).

We have implemented the gravito-hydrodynamic simulation with the Astronomical Multipurpose Software Environment (AMUSE) (Portegies Zwart et al., 2009, 2013; Pelupessy et al., 2013; Portegies Zwart and McMillan, 2018). We couple the gravity and hydrodynamics solvers with a Bridge. We use the classic second-order bridge integration scheme in AMUSE. A higher order Bridge is not needed in our case as *Fi* is a second-order integrator. We set the Bridge timestep to 10 times the hydrodynamics solver timestep (~ 40 days).

3.2 Initial conditions

The initial state of the simulation is generated using the orbital parameters and masses from Peißker et al. (2024), except for the mass of Sgr A*, which is taken from GRAVITY Collaboration et al. (2023). For all initial conditions, see Tab. 1 and Fig. 4.

3.2.1 Disk inner and outer radius

The stability of a disk will depend on the proximity of its inner and outer radii to the binary and the SMBH, respectively.

In order to find the innermost stable orbital radius for our disk, we approximate the system as a binary with total mass m_{bin} with a tertiary orbiting particle with mass m_3 . In such a hierarchical triple system, the binary orbit is referred to as the “inner

¹The binary is not influenced by the disk, because of the low disk mass. This can be verified by comparing Fig. 3 with Fig. A.

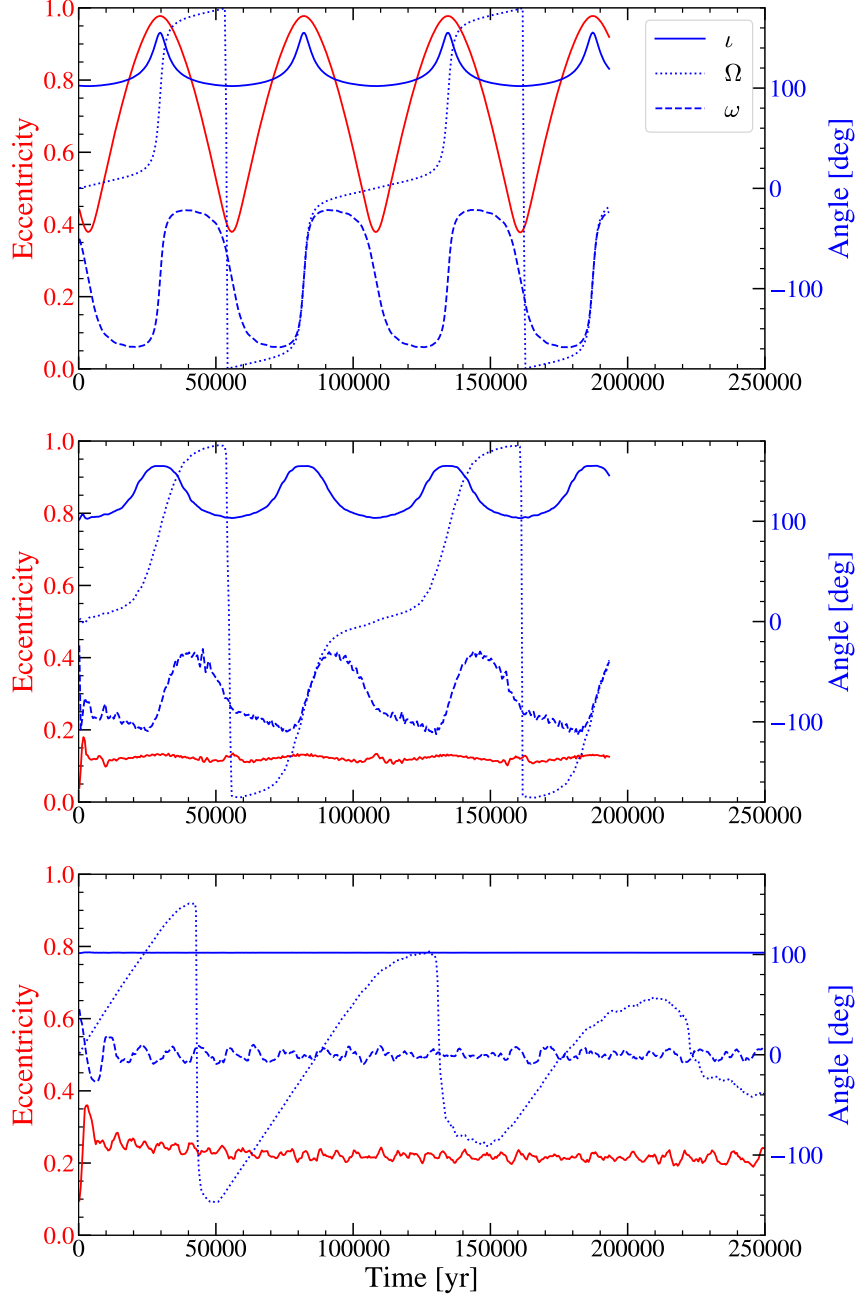


Fig. 3: The vZLK oscillations of the orbital parameters of the binary (upper), circumbinary disk (center) and circumsingle disk (lower) over time. The eccentricity is plotted in red and the spatial angles are plotted in blue. The inclination (ι), longitude of the ascending node (Ω) and argument of periaapse (ω) are indicated by solid, dotted and dashed lines, respectively. In the case of a disk, we plot the median orbital elements of the bound disk particles.

Variable	Value
M_{SgrA^*}	$4.30 \cdot 10^6 M_{\odot}$
M_{D9a}	$2.80 M_{\odot}$
M_{D9b}	$0.73 M_{\odot}$
M_{disk}	$1.6 \cdot 10^{-6} M_{\odot}$
a_{out}	$9.1 \cdot 10^3 \text{ AU}$
e_{out}	0.32
a_{in}	1.59 AU
e_{in}	0.45
i_{mut}	102.55°
ω_{in}	311.75°

Table 1: Initial conditions of the SMBH-D9 system. Masses (M) are given for the primary (D9a) and secondary (D9b) of the binary, its disk and Sgr A*. Eccentricities (e) and semi-major axes (a) are given for the inner binary orbit and the outer orbit around the SMBH. The mutual inclination between these orbits is i_{mut} and the argument of periapse of the inner orbit is ω_{in} .

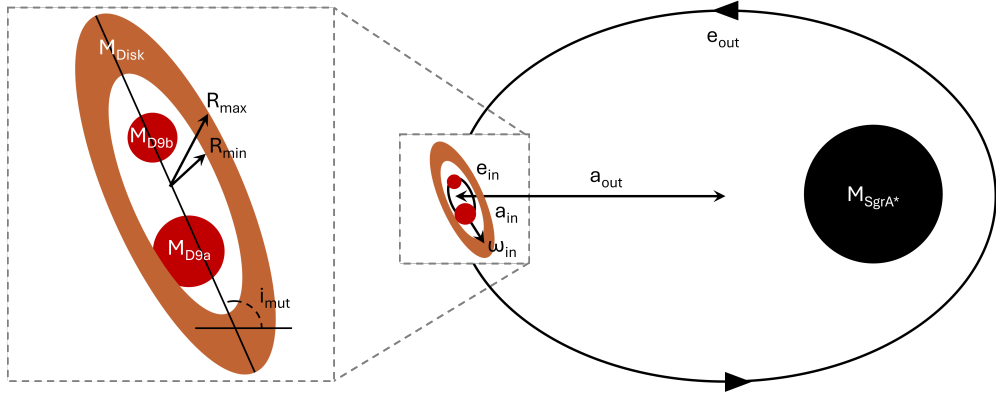


Fig. 4: Sketch of the astrophysical setup. A stellar binary (D9) with circumbinary disk is orbiting a supermassive black hole (Sgr A*). Masses (M), eccentricities (e) and semi-major axes (a) are indicated for the inner binary orbit and the outer orbit around the SMBH. The mutual inclination between these orbits is i_{mut} and the argument of periapse of the inner orbit is ω_{in} .

orbit” with semi-major axis a_{in} and eccentricity e_{in} , while the orbit of the tertiary is called the “outer orbit” with a_{out} and e_{out} the semi-major axis and eccentricity, respectively. Given a mutual inclination of the inner and outer orbits of i_{mut} , the stability criterion is given by [Mardling and Aarseth \(2001\)](#)

$$a_{\text{out}} > 2.8 \cdot \frac{a_{\text{in}}}{1 - e_{\text{out}}} \cdot \left(1 - 0.3 \frac{i_{\text{mut}}}{180^\circ}\right) \cdot \left[\left(1 + \frac{m_3}{m_{\text{bin}}}\right) \cdot \frac{1 + e_{\text{out}}}{\sqrt{1 - e_{\text{out}}}}\right]^{2/5}. \quad (1)$$

Since we assume the disk to be circular and coplanar with the binary, we set $e_{\text{disk}} = 0$ and $i_{\text{mut}} = 0^\circ$. This results in an initial inner disk radius of $R_{\text{min}} = 4.5 \text{ AU}$.

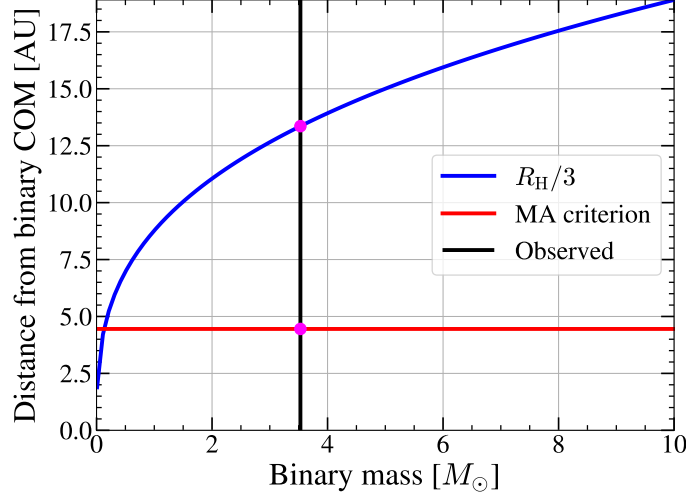


Fig. 5: Minimum and maximum stable radii as a function of total binary mass. The red line indicates the Mardling-Aarseth criterion (Mardling and Aarseth, 2001) for stable orbits in a hierarchical triple. The blue line indicates a third of the Hill radius, outside of which the SMBH will disrupt the disk of D9. The observed binary mass from Peißker et al. (2024) is indicated by the black vertical line and the pink dots denote the intersections. Stable disks must have radii within the region bound by these intersections.

Next, we estimate the outermost stable radius. Inside the Hill sphere of an object, the gravity of the object is dominant over all other objects. As a rule of thumb, orbits are stable up to one-third of the radius of this sphere. The Hill radius of a binary with mass m_{bin} that is orbiting an SMBH with mass M_{SMBH} with an eccentricity e and semi-major axis a is given by (Hill, 1878)

$$R_{\text{H}} = a(1 - e) \left(\frac{m_{\text{bin}}}{m_{\text{bin}} + M_{\text{SMBH}}} \right)^{1/3}. \quad (2)$$

In the case of D9, this means $R_{\text{max}} = \frac{R_{\text{H}}}{3} = 13.4$ AU.

Fig. 5 shows a summary of the discussion above by plotting the stable region as a function of binary mass.

3.2.2 Particle loss and stopping conditions

To find a stable disk configuration, we run multiple simulations with varying inner and outer disk radii. After each run, we increase the inner radius and decrease the outer radius of the disk, based on the number of particles lost in the inner and outer regions of the disk. A lost particle is defined as a particle on a hyperbolic orbit, i.e., with eccentricity $e > 1$. Particles may become re-bound; this is compensated in the simulations.

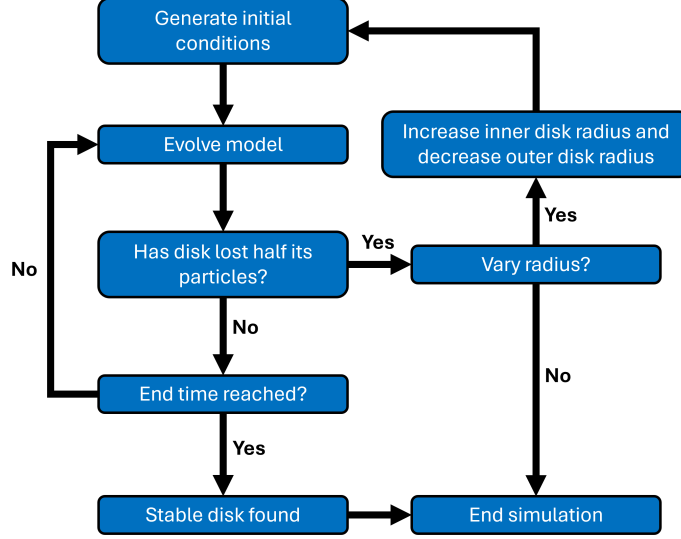


Fig. 6: Flowchart describing the process of finding a stable disk configuration.

We define the half-mass radius (R_{half}) as the radius which encloses half of the mass of the disk. We consider the ratio of particles lost below and above R_{half} and subsequently change R_{min} and R_{max} such that the total disk width shrinks by 10% of the *initial* disk width. That is, let x be the fraction of particles lost at the inner edge. When the additional stopping condition is reached, we set:

$$R_{\text{min,new}} = R_{\text{min,old}} + x \left(\frac{R_{\text{max,initial}} - R_{\text{min,initial}}}{10} \right)$$

$$R_{\text{max,new}} = R_{\text{max,old}} - x \left(\frac{R_{\text{max,initial}} - R_{\text{min,initial}}}{10} \right).$$

This process is repeated until a disk reaches a lifetime of $2.5 \cdot 10^5$ years, or until further shrinking would result in $R_{\text{min}} \geq R_{\text{max}}$. This time limit is set to resolve several vZLK timescales. The described routine is summarized in the flow chart shown in Fig. 6.

4 Discussion

This is, to our knowledge, the first time this system has been studied. Previous studies have been done on the stability of a gaseous disk around Sgr A* (Calderón et al., 2024) or on vZKL oscillations of binaries without a disk that are orbiting an SMBH (Maeda et al., 2023). The vZKL effect has also been studied in circumpriary disks (e.g., Martin et al. 2014; Franchini et al. 2019) in the absence of an SMBH.

4.1 Limitations

Our simulations entail a simplified version of the GC and D9. First, dynamical encounters due to the nearby star cluster are neglected - we study the effect of the SMBH gravitational potential on D9 in isolation. Close encounters with other S-stars are expected to rapidly disrupt the binary-disk system, so with this work we study the stability of the disk in the most optimistic scenario.

Second, we neglect the disk of the Herbig Ae D9 primary. This saves computation time and it is not relevant for the hypothesis we aim to test in this work. We note that a circumprimary disk could be shielded from the gravitational potential of Sgr A* by the secondary, however KL oscillations could still lead to its disruption (Franchini et al., 2019). Further works may investigate this disk.

Third, we model stars as point masses and we neglect stellar winds, Roche lobe overflow or any other process related to stellar evolution. Therefore, we cannot make statements about the proposed imminent merger of D9.

Finally, a fully accurate treatment of the vZKL effect would require a post-Newtonian gravity solver, which we have not implemented.

4.2 Implications

Our results show that a circumbinary disk could survive the gravitational potential of the SMBH and binary and their vZKL oscillations for at least $2.5 \cdot 10^5$ yr.

After an initial drop in the number of bound particles, we observe a periodic disk mass loss in several simulations. We note that the time between the observed periods of temporary stability is roughly equal to the observed vZLK timescale (see Fig. 3). This suggests that the vZLK effect causes periodic short-lived instabilities in the disk that imply a lifetime limitation of the disk based on the vZLK timescale, as the configuration could only survive so many periods of instability.

The vZLK effect is not readily observed in the single-star configuration. This is because the disk quickly loses its flat structure as the disk particle orbits become more isotropic in the absence of a binary.

4.3 Validations

To verify the N-body part of the simulation we plot the energy error of the gravity code in Fig. 7. Because the disk mass is low, we assume that the change in gravitational energy due to the disk is negligible. The maximum relative energy error we observe is $1.98 \cdot 10^{-5}$, indicating reliable results.

We verify the results of the hydrodynamics solver by varying the amount of SPH particles in the disk and checking if the results are similar (Portegies Zwart and McMillan, 2018). We run simulations of our largest possible disk with 10^2 , 10^3 and 10^4 SPH disk particles. Additionally, we run simulations with 10^2 and 10^3 SPH particles using our found quasi-stable disk configuration. We plot the fraction of bound particles for both disk configurations in Fig. 7. We see both disk configurations display similar particle loss curves for all runs, validating our results.

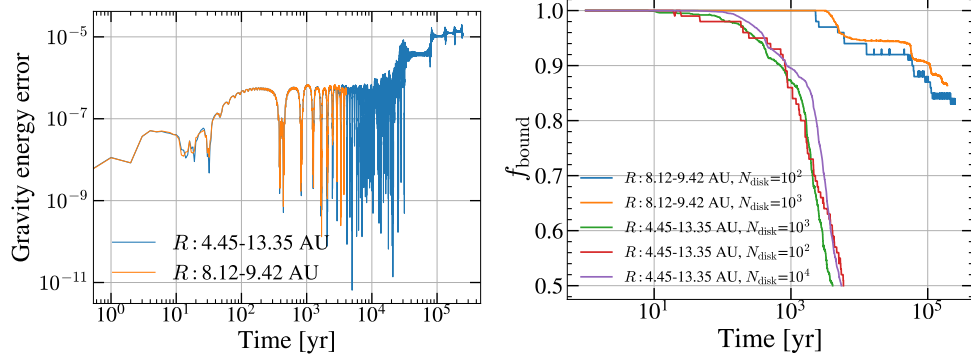


Fig. 7: *Left:* Relative gravity energy error as a function of model time for the default and stable disk configuration. *Right:* Fraction of bound disk particles as a function of model time for the default and stable disk configuration.

5 Conclusion

In the absence of the S-star cluster, there exists a quasi-stable configuration for a circumbinary disk orbiting close to Sgr A*. In this configuration, the disk experiences periodic mass loss driven by vZLK oscillations. Moreover, the disk itself exhibits vZLK oscillations which trace those of the binary orbit.

Supplementary information. The code used in this work can be found in the following GitHub repository: <https://github.com/LucasPouw/amuse-KL>.

Appendix A Gravity code comparison

We test two gravity solvers to determine which gravity code we will use to simulate orbits of the binary and the SMBH: **Huayno** (Jänes et al., 2014) and **Hermite** (Makino, 1991). Since the choice of N-body code only influences the dynamics of the SMBH-binary system, we omit the disk in this test. The evolution of the orbital elements of the binary orbit can be found in Figure A1. Both integrators show clear oscillations in eccentricity and inclination. However, the amplitude and period of the oscillations are not the same across the two integrators. **Huayno** is the faster code and we deem its accuracy sufficient for our purposes.

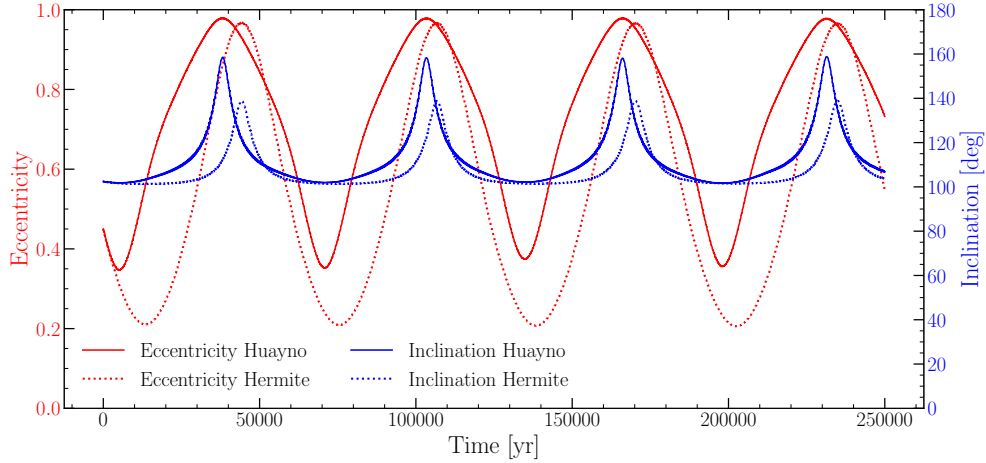


Fig. A1: Comparison of the **Hermite** (dotted lines) and **Huayno** (solid lines) N-Body codes. We show the time evolution of the eccentricity (red lines) and inclination (blue lines) of the binary orbit.

References

- Calderón, D., Cuadra, J., Russell, C.M.P., Burkert, A., Rosswog, S., Balakrishnan, M.: The formation and stability of a cold disc made out of stellar winds in the Galactic Centre. arXiv e-prints, 2411–00100 (2024) <https://doi.org/10.48550/arXiv.2411.00100> arXiv:2411.00100 [astro-ph.GA]
- Franchini, A., Martin, R.G., Lubow, S.H.: Misaligned accretion disc formation via Kozai-Lidov oscillations. Mon. Not. R. Soc. **485**(1), 315–325 (2019) <https://doi.org/10.1093/mnras/stz424> arXiv:1902.04090 [astro-ph.EP]
- GRAVITY Collaboration, Abuter, R., Aymar, N., Amaro Seoane, P., Amorim, A., Bauböck, M., Berger, J.P., Bonnet, H., Bourdarot, G., Brandner, W., Cardoso, V.,

- Clénet, Y., Davies, R., de Zeeuw, P.T., Dexter, J., Drescher, A., Eckart, A., Eisenhauer, F., Feuchtgruber, H., Finger, G., Förster Schreiber, N.M., Foschi, A., Garcia, P., Gao, F., Gelles, Z., Gendron, E., Genzel, R., Gillessen, S., Hartl, M., Haubois, X., Haussmann, F., Heißel, G., Henning, T., Hippler, S., Horrobin, M., Jochum, L., Jocu, L., Kaufer, A., Kervella, P., Lacour, S., Lapeyrère, V., Le Bouquin, J.-B., Léna, P., Lutz, D., Mang, F., More, N., Ott, T., Paumard, T., Perraut, K., Perrin, G., Pfuhl, O., Rabien, S., Ribeiro, D.C., Sadun Bordoni, M., Scheithauer, S., Shang-guan, J., Shimizu, T., Stadler, J., Straub, O., Straubmeier, C., Sturm, E., Tacconi, L.J., Vincent, F., von Fellenberg, S., Widmann, F., Wielgus, M., Wieprecht, E., Wiezorrek, E., Woillez, J.: Polarimetry and astrometry of NIR flares as event horizon scale, dynamical probes for the mass of Sgr A*. *Astron. Astrophys.* **677**, 10 (2023) <https://doi.org/10.1051/0004-6361/202347416> [arXiv:2307.11821](https://arxiv.org/abs/2307.11821) [astro-ph.GA]
- Grant, S.L., Espaillat, C.C., Brittain, S., Scott-Joseph, C., Calvet, N.: Tracing Accretion onto Herbig Ae/Be Stars Using the Br γ Line. *Astrophys. J.* **926**(2), 229 (2022) <https://doi.org/10.3847/1538-4357/ac450a> [arXiv:2112.10428](https://arxiv.org/abs/2112.10428) [astro-ph.SR]
- Gerritsen, J.P.E., Icke, V.: Star formation in N-body simulations. I. The impact of the stellar ultraviolet radiation on star formation. *Astron. Astrophys.* **325**, 972–986 (1997)
- Hill, G.W.: Researches in the lunar theory. *American Journal of Mathematics* **1**(1), 5–26 (1878). Accessed 2025-01-11
- Hernquist, L., Katz, N.: TREESPH: A Unification of SPH with the Hierarchical Tree Method. *Astrophys. J. Supp.* **70**, 419 (1989) <https://doi.org/10.1086/191344>
- Jänes, J., Pelupessy, I., Portegies Zwart, S.: A connected component-based method for efficiently integrating multi-scale N-body systems. *Astron. Astrophys.* **570**, 20 (2014) <https://doi.org/10.1051/0004-6361/201423831> [arXiv:1407.7105](https://arxiv.org/abs/1407.7105) [astro-ph.IM]
- Kozai, Y.: Secular perturbations of asteroids with high inclination and eccentricity. *Astron. J.* **67**, 591–598 (1962) <https://doi.org/10.1086/108790>
- Lidov, M.L.: The evolution of orbits of artificial satellites of planets under the action of gravitational perturbations of external bodies. *Planet. Space Sci.* **9**(10), 719–759 (1962) [https://doi.org/10.1016/0032-0633\(62\)90129-0](https://doi.org/10.1016/0032-0633(62)90129-0)
- Mardling, R.A., Aarseth, S.J.: Tidal interactions in star cluster simulations. *Mon. Not. R. Soc.* **321**(3), 398–420 (2001) <https://doi.org/10.1046/j.1365-8711.2001.03974.x>
- Makino, J.: Optimal Order and Time-Step Criterion for Aarseth-Type N-Body Integrators. *Astrophys. J.* **369**, 200 (1991) <https://doi.org/10.1086/169751>
- Maeda, K.-i., Gupta, P., Okawa, H.: Dynamics of a binary system around a super-massive black hole. *Phys. Rev. D* **107**(12), 124039 (2023) <https://doi.org/10.1103/>

[PhysRevD.107.124039](#) [arXiv:2303.16553](#) [gr-qc]

Muzerolle, J., Hartmann, L., Calvet, N.: A Brgamma Probe of Disk Accretion in T Tauri Stars and Embedded Young Stellar Objects. *Astron. J.* **116**(6), 2965–2974 (1998) <https://doi.org/10.1086/300636>

Martin, R.G., Nixon, C., Lubow, S.H., Armitage, P.J., Price, D.J., Doğan, S., King, A.: The Kozai-Lidov Mechanism in Hydrodynamical Disks. *Astrophys. J. Lett.* **792**(2), 33 (2014) <https://doi.org/10.1088/2041-8205/792/2/L33> [arXiv:1409.1226](#) [astro-ph.EP]

Portegies Zwart, S., McMillan, S.: *Astrophysical Recipes; The Art of AMUSE*, (2018). <https://doi.org/10.1088/978-0-7503-1320-9>

Portegies Zwart, S., McMillan, S., Harfst, S., Groen, D., Fujii, M., Nualláin, B.Ó., Glebbeek, E., Hoggie, D., Lombardi, J., Hut, P., Angelou, V., Banerjee, S., Belkus, H., Fragos, T., Fregeau, J., Gaburov, E., Izzard, R., Jurić, M., Justham, S., Sottoriva, A., Teuben, P., van Bever, J., Yaron, O., Zemp, M.: A multi-physics and multiscale software environment for modeling astrophysical systems. *New Astron.* **14**(4), 369–378 (2009) <https://doi.org/10.1016/j.newast.2008.10.006> [arXiv:0807.1996](#) [astro-ph]

Portegies Zwart, S., McMillan, S.L.W., van Elteren, E., Pelupessy, I., de Vries, N.: Multi-physics simulations using a hierarchical interchangeable software interface. *Computer Physics Communications* **184**(3), 456–468 (2013) <https://doi.org/10.1016/j.cpc.2012.09.024> [arXiv:1204.5522](#) [astro-ph.IM]

Pelupessy, F.I., van Elteren, A., de Vries, N., McMillan, S.L.W., Drost, N., Portegies Zwart, S.F.: The Astrophysical Multipurpose Software Environment. *Astron. Astrophys.* **557**, 84 (2013) <https://doi.org/10.1051/0004-6361/201321252> [arXiv:1307.3016](#) [astro-ph.IM]

Pelupessy, F.I., van der Werf, P.P., Icke, V.: Periodic bursts of star formation in irregular galaxies. *Astron. Astrophys.* **422**, 55–64 (2004) <https://doi.org/10.1051/0004-6361:20047071> [arXiv:astro-ph/0404163](#) [astro-ph]

Peißker, F., Zajacek, M., Labadie, L., Bordier, E., Eckart, A., Melamed, M., Karas, V.: A binary system in the S cluster close to the supermassive black hole Sagittarius A*. *arXiv e-prints*, 2412–12727 (2024) <https://doi.org/10.48550/arXiv.2412.12727> [arXiv:2412.12727](#) [astro-ph.GA]

von Zeipel, H.: Sur l’application des séries de M. Lindstedt à l’étude du mouvement des comètes périodiques. *Astronomische Nachrichten* **183**(22), 345 (1910) <https://doi.org/10.1002/asna.19091832202>